Regulation of Deactivation by an Amino Terminal Domain in *Human Ether-à-go-go–related Gene* Potassium Channels

Jinling Wang, Matthew C. Trudeau, Angelina M. Zappia, and Gail A. Robertson

From the Department of Physiology, University of Wisconsin-Madison Medical School, Madison, Wisconsin 53706

ABSTRACT Abnormalities in repolarization of the cardiac ventricular action potential can lead to life-threatening arrhythmias associated with long QT syndrome. The repolarization process depends upon the gating properties of potassium channels encoded by the *human ether-à-go-go–related gene* (HERG), especially those governing the rate of recovery from inactivation and the rate of deactivation. Previous studies have demonstrated that deletion of the NH_2 terminus increases the deactivation rate, but the mechanism by which the NH_2 terminus regulates deactivation in wild-type channels has not been elucidated. We tested the hypothesis that the HERG NH_2 terminus slows deactivation by a mechanism similar to N-type inactivation in *Shaker* channels, where it binds to the internal mouth of the pore and prevents channel closure. We found that the regulation of deactivation by the HERG NH_2 terminus bears similarity to *Shaker* N-type inactivation in three respects: (*a*) deletion of the NH_2 terminus slows C-type inactivation; (*b*) the action of the NH_2 terminus is sensitive to elevated concentrations of external K^+, as if its binding along the permeation pathway is disrupted by K^+ influx; and (*c*) *N*-ethylmaleimide, covalently linked to an aphenotypic cysteine introduced within the S4–S5 linker, mimics the N deletion phenotype, as if the binding of the NH_2 terminus to its receptor site were hindered. In contrast to N-type inactivation in *Shaker*, however, there was no indication that the NH_2 terminus blocks the HERG pore. In addition, we discovered that separate domains within the NH_2 terminus mediate the slowing of deactivation and the promotion of C-type inactivation. These results suggest that the NH_2 terminus stabilizes the open state and, by a separate mechanism, promotes C-type inactivation.

KEY WORDS: ion channels • gating • inactivation • cysteine modification

INTRODUCTION

The *human ether-à-go-go–related gene* (HERG)[1] encodes a subunit of the ion channels underlying cardiac I_{Kr} (Sanguinetti et al., 1995; Trudeau et al., 1995), a potassium current that contributes to the terminal repolarization of the ventricular action potential (Sanguinetti and Jurkewicz, 1990). The HERG polypeptide exhibits structural similarities to members of the S4-containing superfamily of ion channels (Warmke and Ganetzky, 1994) and its behavior can be described by typical gating characteristics such as a sigmoidal time course of activation (Trudeau et al., 1995) and C-type inactivation (Schönherr and Heinemann, 1996; Smith et al., 1996). Despite these similarities, HERG currents look different from other K^+ currents because of the temporal relationships among these gating transitions: at positive voltages, channels inactivate quickly, spending little time in the open state; at repolarizing voltages, deactivation is slow, resulting in relatively greater occupancy of the open state as channels recover from inactivation (Sanguinetti et al., 1995; Trudeau et al., 1995; compare Shibasaki, 1987). Scheme I shows a simple model in which C represents the closed state, O the open state, and I the inactivated state. As a consequence of the fast inactivation and slow deactivation, the corresponding macroscopic currents reach their maximum amplitude not at positive voltages like most voltage-gated channels, but instead at more negative voltages during a subsequent repolarizing step. The resulting profile of I_{Kr} during the cardiac action potential, inferred from expression studies of HERG in heterologous systems (Zhou et al., 1998) and modeled for native tissues (Zeng et al., 1995), is a resurgent current that is suppressed at the peak of the action potential but rebounds during repolarization. The timing and amplitude of this resurgent current are thus determined by the rate of recovery from inactivation and the subsequent rate of deactivation during the repolarization phase of the cardiac action potential.

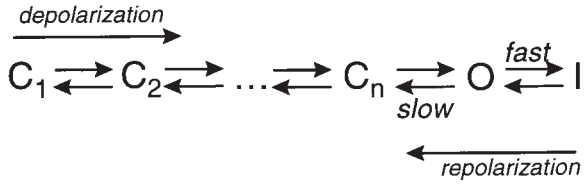

(SCHEME I)

Address correspondence to Dr. G.A. Robertson, Department of Physiology, 129 S.M.I., University of Wisconsin-Madison Medical School, 1300 University Ave., Madison, WI 53706. Fax: 608-265-5512; E-mail: robertson @physiology.wisc.edu

[1]*Abbreviations used in this paper:* HERG, *human ether-à-go-go–related gene*; NEM, *N*-ethylmaleimide; WT, wild type.

Previous studies have demonstrated that the rate of deactivation in HERG channels is dramatically increased when the NH_2 terminus is deleted (Schönherr and Heinemann, 1996; Spector et al., 1996). Isoforms with truncated or alternative, short N termini and correspondingly fast deactivation rates are encoded by splice variants of Merg1, the mouse ortholog to HERG (Lees-Miller et al., 1997; London et al., 1997). The same splice variants arise from the HERG locus (London et al., 1998). Thus, the NH_2 terminus regulates deactivation gating and represents a mechanism by which functional diversity is generated in HERG and related channels.

In this study, we tested the hypothesis that the NH_2 terminus of the HERG long isoform slows deactivation by a foot-in-the-door mechanism similar to effects obtained with tetraethylammonium (Armstrong, 1966) and mediated by the NH_2 terminus of *Shaker* channels (Demo and Yellen, 1991). Our results suggest that the NH_2 terminus binds to a site near the internal mouth of the pore, where it is sensitive to elevated external K^+ ions and to modification by *N*-ethylmaleimide (NEM). Despite several properties reminiscent of the mechanism of N-type inactivation in *Shaker* channels, including an interaction with C-type inactivation (Hoshi et al., 1991; Baukrowitz and Yellen, 1995), we also find important differences, consistent with the lack of primary structural similarity of the N termini and their receptor sites in these distantly related channels. This study reveals a complexity in the function of the HERG NH_2 terminus and raises new questions pertinent to other voltage-gated K^+ channels as well.

METHODS

Construction of Deletion and Point Mutations

The HERG NH_2-terminal deletion clone Δ2-354 was constructed using a one-step PCR. The forward primer contained sequence for a BamHI site, the Kozak consensus sequence, and the codon for the initiating methionine followed by an 18-base sequence corresponding to the residues immediately upstream of those encoding the putative S1 region of the channel. The reverse primer crossed a BglII restriction site downstream. The resulting PCR product was a DNA fragment missing the coding sequence for amino acids 2–354. This fragment was purified and ligated into the parent construct using BamHI and BglII sites. The HERG S620T (Herzberg et al., 1998) and all the cysteine mutants were constructed using a two-step PCR-based mutagenesis method as previously described (Landt et al., 1990). The final PCR fragment was cut with the appropriate restriction enzymes and ligated into the wild-type construct at the corresponding sites. The ligation products were transformed into JM109 cells. Plasmid DNA was purified from the cells and amplified sequences and subcloning sites were verified by ABI automated sequencing (University of Wisconsin-Madison Biotechnology Center).

Preparation of Oocytes and RNA Synthesis and Injection

Oocytes were removed from anesthetized frogs (*Xenopus laevis*; Nasco, Fort Atkinson, WI) through a small abdominal incision according to procedures approved by the University of Wisconsin Research Animals Resource Center and the National Institutes of Health (NIH). The follicular membranes were removed after collagenase treatment (Collagenase B; Boehringer Mannheim Biochemicals, Indianapolis, IN) and, in some cases, by an osmotic shock procedure (Pajor et al., 1992). RNA was synthesized from linearized template using mMESSAGE mMachine kit (Ambion Inc., Austin, TX). RNA was diluted in sterile water to different ratios to give upon expression an optimal 2–10 μA outward current (the maximal current obtained during a series of depolarizing steps, usually at −10 or 0 mV). Oocytes were cultured at 18°C in storage solution (96 mM NaCl, 2 mM KCl, 1 mM $MgCl_2$, 1.8 mM $CaCl_2$, 5 mM HEPES, supplemented with 10 μg/ml gentamicin and 1 mg/ml BSA, pH 7.4).

Current Recording and Data Analysis

Currents were recorded using a two-electrode voltage clamp (OC-725C; Warner Instruments, Hamden, CT) and pClamp 6.0.3 software (Axon Instruments, Foster City, CA). PClamp 6.0.3 and Origin 4.1 (Microcal Software, Inc., Northampton, MA) were used for data analysis and generating plots. The resistance of the electrodes was 0.5–1 MΩ in 2 M KCl. The bath solutions contained varying amounts of K^+ but the solution was kept isosmolar by balancing with *N*-methyl glutamine (NMG) so that the total [KCl + NMG] = 98 mM (no Na^+ was used). One exception was in the "knock-off" experiments in which high concentrations of K^+ were used (as described in the Fig. 4 legend) and the solution osmolarities were different for different K^+ concentrations. No oocyte shrinkage was observed under these conditions and recordings were generally completed within 5 min. In addition, the solutions contained 1 mM $MgCl_2$, 0.3 mM $CaCl_2$, 5 mM HEPES, pH 7.4. Holding potential was −80 mV and all recordings were done at room temperature, roughly 25°C. Data were routinely discarded if the leak exceeded 10% of the maximum conductance of the expressed currents, but for all the data in this study, the leak currents stepping from −80 to −100 mV were <0.2 μA, << 1% of the maximum conductance of the expressed currents, and therefore no leak subtraction was used. Sample numbers (*n*'s) refer to the number of individual oocytes recorded.

Time constants (τ's) for the currents were measured using Clampfit. Data were digitized at 2 or 4 kHz and unfiltered. Deactivation τ's were derived from a Chebyshev fit to the deactivating current of the equation $y = A_0 + A_1 e^{-t/\tau 1} + A_2 e^{-t/\tau 2}$. Fitting began within 5 ms of the peak of the tail current, with the first cursor of the fitting window advanced to the first point in time that did not force a fit to the recovery phase; the second cursor was at the end of the 1.5-s pulse. The deactivation traces were best fit with two τ's. At more negative voltages, most of the current was described by a single, fast deactivation tau for both channel types (Table I) such that $\tau_{fast} \cong 1/\alpha + \beta$, the sum of the activation and deactivation rates, respectively; since activation is negligible at negative voltages, $\tau_{fast} \cong 1/\beta$.

The inactivation time constant was similarly derived from a fit of the equation $y = Ae^{-t/\tau}$ to the inactivating current. In this case, the fitting window began as soon as the clamp settled, ~2 ms, and continued to the end of the 300-ms pulse.

The activation time constant was derived using an envelope of tails protocol (Fig. 1 *D, inset*; Trudeau et al., 1995; Wang et al., 1997). This protocol consists of depolarizing steps, each followed by repolarization to −100 mV, given in successive increments of either 10 (for voltage commands to 40 and 60 mV) or 100 (for −20, 0, and 20 mV) ms. The deactivating phase of tail currents elicited for each trace was fit with a double exponential function and back extrapolated to the initial time point of repolarization ($t = 0$). The fitting window was the same as that used for the stan-

TABLE I

Fraction of Fast Deactivating Component in the Tail Currents

V	WT	Δ2-354
mV		
−40	0.24 ± 0.04	0.16 ± 0.04
−50	0.33 ± 0.05	0.30 ± 0.04
−60	0.46 ± 0.05	0.34 ± 0.05
−70	0.58 ± 0.05	0.47 ± 0.04
−80	0.73 ± 0.04	0.56 ± 0.03
−90	0.82 ± 0.03	0.68 ± 0.02
−100	0.85 ± 0.02	0.76 ± 0.02
−110	0.89 ± 0.03	0.84 ± 0.02
−120	0.90 ± 0.02	0.92 ± 0.02

Tail currents are fit with double exponential function $y = A_0 + A_f e^{-t/\tau f} + A_s e^{-t/\tau s}$. Percentage of fast component is calculated as $A_f/(A_f + A_s)$.

dard tail current protocol described above for deactivation. The current measured at $t = 0$ is assumed to be proportional to the total number of channels that have undergone the transition from the closed to the open state. The resulting values were plotted against the duration of depolarization and fitted to a single exponential function to obtain the time constant of activation. These activating currents are actually sigmoidal in nature and so the fit to a single exponential represents a simplifying approximation.

Chemical Modification of Cysteine Mutants

5 mM NEM (Sigma Chemical Co., St. Louis, MO) was added to the bath solution after one control recording under the two-electrode voltage clamp configuration. The final concentration achieved in the bath solution was ~2 mM. Before subsequent recordings, oocytes were bathed for 15 min to allow the reagent to permeate the membrane. Oocytes were held at −80 mV during the incubation period.

RESULTS

The NH_2 Terminus Slows Deactivation and Promotes C-Type Inactivation

The amino (NH_2) terminus of HERG has multiple effects on macroscopic gating parameters. Using a deletion mutant lacking most of the sequence preceding the S1 domain (Δ2-354), we confirmed previous reports that removing the NH_2 terminus increases the deactivation rate (Spector et al., 1996; Schönherr and Heinemann, 1996). Fig. 1 *A* shows families of deactivating currents from wild-type HERG and Δ2-354 channels. Comparison of these currents shows that both recovery from inactivation and deactivation are much faster in Δ2-354 (Fig. 1, *A* and *B*). To quantitate the differences in deactivation rates, the time constants (τ's) of deactivation are extracted from a double exponential fit to the decaying phase of the tail current. The plot shows that both time constants are ~10-fold reduced when the NH_2 terminus is deleted, reflecting a corresponding increase in deactivation rate (Fig. 1 *C*; see METHODS). Thus, the NH_2 terminus slows the deactivation process in wild-type channels. In contrast, the activation rates measured using an envelope of tails protocol (see METHODS) are not significantly altered by the NH_2 terminus deletion (Fig. 1 *D*), indicating that neither the free energy of the closed state nor the energy of the activation barrier is affected by the NH_2 terminus. This specific effect on deactivation rate suggests that, during activation, the NH_2 terminus interacts selectively with the open state, lowering its free energy. Since the channel cannot close until the NH_2 terminus dissociates, the overall rate of deactivation is slowed.

The NH_2 terminus also modulates the inactivation rate. When the NH_2 terminus is deleted, C-type inactivation is slowed and is less complete than in wild-type channels (Fig. 2, *A* and *B*). This result indicates that the NH_2 terminus promotes and stabilizes C-type inactivation by lowering the energy barrier of the transition between the open and inactivated states and by lowering the free energy (ΔG) of the C-type–inactivated state relative to the open state. The NH_2 terminus stabilizes the inactivated state by an average of −0.67 kcal/mol ± 0.14 (mean ± SD) relative to the open state without changing the voltage dependence of inactivation (Fig. 2 *C*, see legend for calculation of ΔG). Consistent with more complete steady state inactivation, the normalized current–voltage relation shows less outward current (more inward rectification) in the wild-type channel compared with Δ2-354 at more positive voltages (Fig. 2 *D*). At more negative voltages, the wild-type current is larger, as predicted by the slower deactivation and stabilization of the open state by the NH_2 terminus (compare Fig. 1). The stabilization of the C-type–inactivated state and the slowing of deactivation are reminiscent of N-type inactivation in *Shaker*-related channels, in which both effects are attributed to a pore-binding mechanism by the NH_2-terminal domain (Hoshi et al., 1990, 1991; Zagotta et al., 1990; Baukrowitz and Yellen, 1995).

Modulation of Deactivation by the NH_2 Terminus Is Not Due to Stabilization of Inactivation

By lowering the free energy of the inactivated state, the NH_2 terminus might be expected slow the rate of recovery from inactivation and, by mass action, the apparent rate of deactivation. In this way, all effects of the NH_2 terminus could be attributable to the stabilization of the inactivated state, with no need to invoke an additional mechanism for the slowing of deactivation. To distinguish such an apparent rate change from a direct effect on the deactivation transition, we measured changes in the deactivation time constants brought about by removing the NH_2 terminus in channels lacking C-type inactivation (S620T; Herzberg et al., 1998). As shown in Fig. 3 *A*, the deactivation rate increases when the NH_2 terminus is removed from the S620T mutant. The differences in deactivation τ's caused by

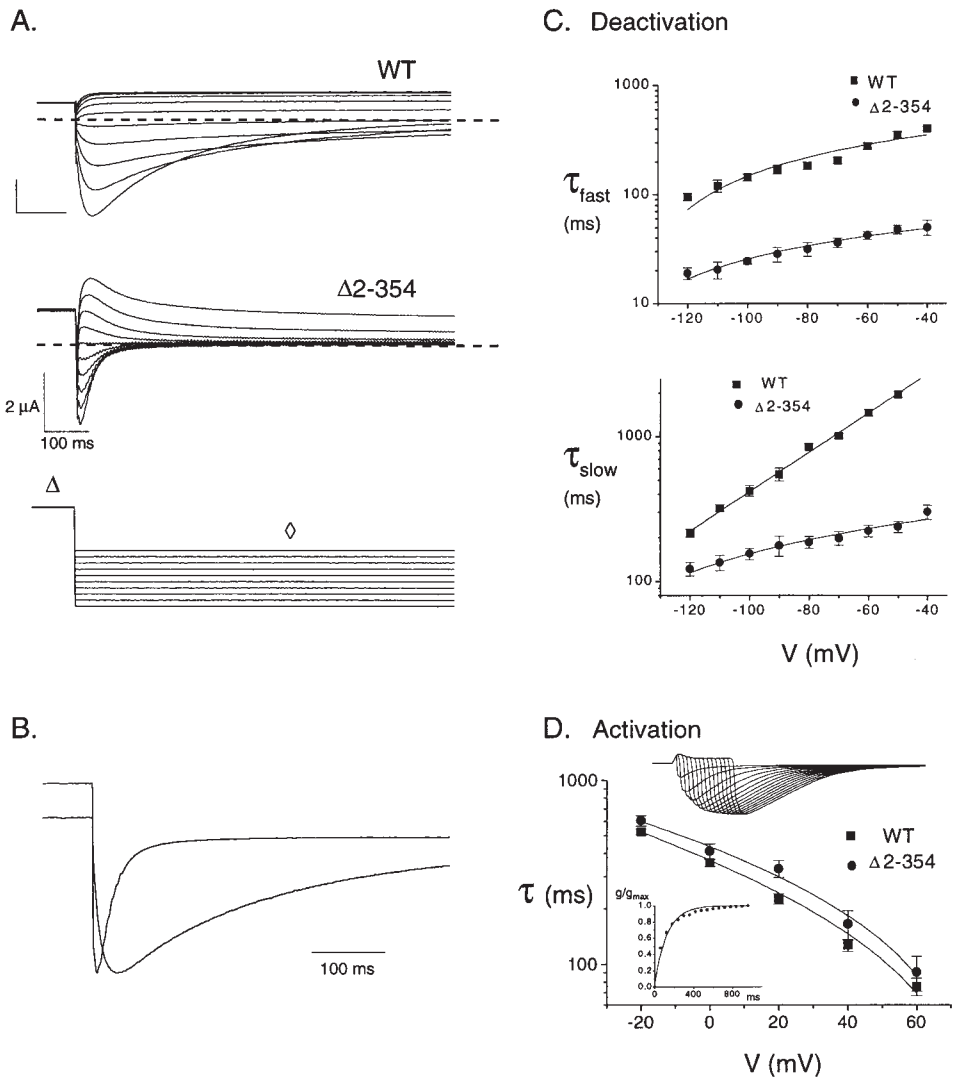

FIGURE 1. The HERG NH_2 terminus slows deactivation but does not alter activation kinetics. (*A*) Families of tail currents from HERG wild-type (WT) and N deletion (Δ2-354) channels. Channels were allowed to fully activate and inactivate during a 3-s depolarizing pulse to 60 mV, only part of which is shown (*Δ*); during a subsequent step to potentials ranging from −120 to −40 mV (◇), currents recovered from inactivation, and then deactivated. The holding potential was −80 mV. The zero current level is indicated by the dashed line. (*B*) Scaled tail currents evoked by a −100-mV repolarizing pulse from the experiment in *A* show that Δ2-354 channels deactivate faster than WT channels. (*C*) Fast (*top*) and slow (*bottom*) deactivation time constants obtained from double exponential fits to the closing phase of the tail currents plotted vs. repolarizing voltage values (see METHODS) for wild-type and Δ2-354 channels ($n \geq 10$). Each point represents the mean, and the error bars are SEM for this and all subsequent figures. (*D*) Activation time constants for WT and Δ2-354 channels are plotted for different voltages. There is no significant difference between these values for WT and Δ2-354 channels ($P \geq 0.58$ at confidence interval of 0.05 in one-way analysis of variance test). Top inset shows a series of currents evoked by the envelope of tails protocol to measure time-dependent increases in conductance, as described in METHODS, with a step to 40 mV (Trudeau et al., 1995; Wang et al., 1997); bottom inset shows exponential fit to resulting conductance vs. time plot ($n = 6$).

removal of the NH_2 terminus are indistinguishable from those in the wild-type background (Fig. 3 *B*). This result indicates that regulation of the apparent deactivation rate by the NH_2 terminus is a direct effect on channel closing and can occur even when the inactivation mechanism is disabled.

Modulation of Deactivation by the NH_2 Terminus Is Sensitive to Elevated $[K]_o$

We tested the hypothesis that the NH_2 terminus in HERG slows deactivation by binding to the internal mouth of the pore. Based on this hypothesis, the NH_2 terminus is expected to lie along the permeation pathway, and the deactivation rate should be sensitive to increases in K^+ influx that destabilize the NH_2 terminus residency there (compare Armstrong, 1966; MacKinnon and Miller, 1988). Fig. 4 *A* shows that deactivation rate increases with elevated external potassium ($[K^+]_o$). This is shown quantitatively as a gradual decrease in the value of the deactivation time constants as $[K^+]_o$ is elevated, an effect not observed when the NH_2 terminus is deleted and thus attributed to disruption of the NH_2 terminus action rather than nonspecific effects of changes in osmolarity (Fig. 4 *B*). Plotting the fractional change in the rate of deactivation ($1/\tau$) as a function of $[K^+]_o$ reveals a sharp dose–response relationship with a $K_{1/2}$ of 130.48 ± 2.16 mM and a Hill coefficient of 5.36 ± 0.69 (Fig. 4 *C*). This destabilization could occur by an allosteric modification of the NH_2 terminus binding site by elevated external K^+ ions, or by a "knock-off" effect whereby permeating K^+ ions directly destabilize the binding of the NH_2 terminus. The value of the Hill coefficient obtained together with the

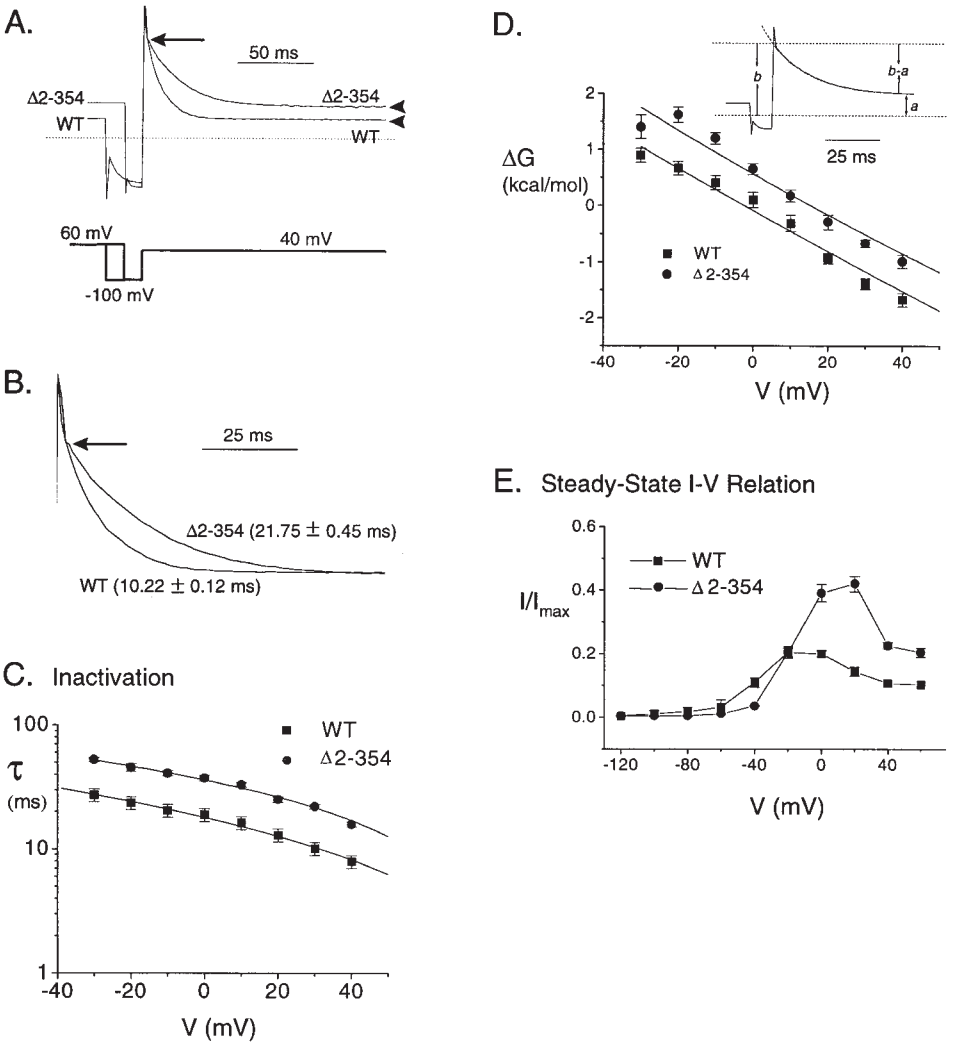

FIGURE 2. The HERG NH_2 terminus promotes C-type inactivation. (*A*) Inactivating current traces scaled to the peak current from WT and Δ2-354 channels generated using the three-pulse protocol: channels are allowed to fully activate and inactivate during a 3-s prepulse to 60 mV; a subsequent, brief repolarizing pulse to −100 mV allows channels to recover; near the peak of this tail current before deactivation becomes apparent, a third pulse to one of a range of voltages is given to drive channels from the open into the inactivated state (40 mV for the traces shown). The repolarizing pulse is 35 ms in duration for WT, 15 ms for Δ2-354. (Based on our fits, we calculate that recovery is 99.02 ± 0.72%, $n = 14$, complete for WT and 99.50 ± 0.29%, $n = 8$ complete for Δ2-354 at the peak of the tail current; i.e., end of recovery phase. This was determined by fitting the recovery phase of the tail currents with a single exponential of the form $y = A_0 + Ae^{-t/\tau}$. The fit, which in most cases followed very closely to the peak currents, was extended beyond the peak to a plateau. The current level of the plateau was considered to represent the full recovery from inactivation. The amplitude of the peak tail current was normalized to this value to give the percentage of recovery, the mean values for which are reported above.) Thus, an inactivating current is measured in relative isolation from other kinetic components. Arrowheads point to the steady state inactivation level of WT and Δ2-354 channels. The dashed line indicates the zero current level. The capacitance artifact (~2 ms) ends at the arrow. Capacitance artifacts are also shown at the beginning of the tail currents upon repolarization. (*B*) Currents from *A* scaled to peak and minimum to show the difference in time course. Time constants extracted from single exponential fits are shown along with the error of the fit. The arrow corresponds to the settling of the clamp as shown in *A*. (*C*) Inactivation time constants extracted from single exponential fits to the inactivating current illustrated in *A* are plotted at different voltages ($n \geq 10$). (*D*) Change in free energy as a function of voltage shows that deletion of the NH_2 terminus increases the free energy of the inactivated state relative to the open state ($n = 6$). The free energy change associated with open to inactivated transition can be calculated as $\Delta G_{O\leftrightarrow I} = -RT\ln K_{O\leftrightarrow I} = -RT\ln(I/O) = RT\ln(O/I)$, where ΔG is the difference in free energy between the open and closed states. I and O are the fraction of channels in the inactivated and open states, respectively, R is the gas constant and T is the temperature. The fraction of open and inactivated channels are measured from the inactivation current as illustrated in the inset: the instantaneous outward current level, indicated as *b*, reflects the total number of channels that are open and ready to undergo the open to inactivated transition. The value for *b* is determined by fitting the inactivating current with a single exponential function and extrapolating back to the moment of the voltage change; the fit departs from the recorded current during the capacitive artifact, which has a duration of ~2 ms. The steady state current level (the channels remaining in O) is indicated as *a*. Thus, the number of inactivated channels can be calculated as $(b - a)$. Then, at any given voltage, $\Delta G_{O\leftrightarrow I} = RT\ln(O/I) = RT\ln[b/(b - a)]$. The example shown is a Δ2-354 current. (*E*) Normalized steady state outward current–voltage relationships for WT and Δ2-354 channels ($n = 6$). All outward currents are normalized to the maximal tail current level evoked at −100 mV subsequent to a 3-s step to 60 mV, which represents the channel expression level for each oocyte assuming the same single-channel conductance for the two constructs.

associated error range suggest that a minimum of five or six K^+ ions are required for this effect.

The increase in deactivation rate is consistent with the interpretation that elevated K^+ destabilizes the binding of the NH_2 terminus. At saturating K^+ concentrations, this corresponds to a destabilizing energy of 0.55 kcal/mol at −100 mV, as follows: the change in free energy for the transition from the closed to the open

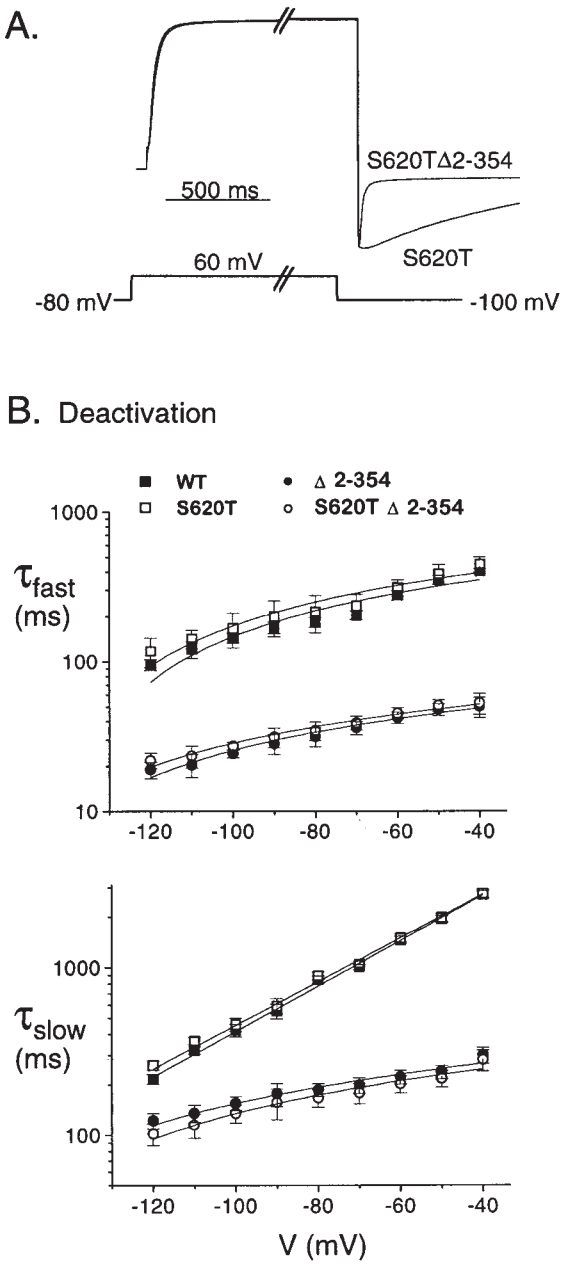

FIGURE 3. NH_2 terminus regulation of deactivation is independent of the inactivation process. (*A*) Scaled outward currents from S620T and S620T Δ2-354 channels show that deleting the NH_2 terminus increases deactivation rate even in the absence of C-type inactivation. (*B*) Fast and slow deactivation time constants for WT ($n \geq 10$), Δ2-354 ($n \geq 10$), S620T ($n = 6$), and S620TΔ2-354 ($n = 6$) channels showing that the change in deactivation rate due to deletion of the NH_2 terminus is the same in the absence of C-type inactivation as in the wild-type background.

conformations is $\Delta G = -RT\ln K = RT\ln(\beta/\alpha)$, where K is the equilibrium constant for the transition, and α and β are the activation and deactivation rates, respectively. The disruption of the NH_2 terminus action caused by elevating external K^+ ("high K^+" = 150 mM) is determined relative to the free energy values of the wild-type channels and Δ2-354 channels in control solutions:

$$\Delta G_{WT} = -RT\ln K_{WT} = RT\ln(\beta/\alpha)_{WT}$$

$$\Delta G_{\Delta 2\text{-}354} = -RT\ln K_{\Delta 2\text{-}354} = RT\ln(\beta/\alpha)_{\Delta 2\text{-}354}$$

$$\Delta G_{\text{high } K^+} = -RT\ln K_{\text{high } K^+} = RT\ln(\beta/\alpha)_{\text{high } K^+}$$

$\beta \cong 1/\tau_{fast}$ since $\tau = 1/(\alpha + \beta)$, α is negligible at −100 mV and 85% of the deactivation current is described by the fast time constant (see Table I and METHODS). The change in free energy caused by deleting the NH_2 terminus can be calculated as follows:

$$\Delta G_{WT} - \Delta G_{\Delta 2\text{-}354} = -RT\ln(\beta_{WT}/\beta_{\Delta 2\text{-}354})$$

$$= RT\ln(\tau_{WT}/\tau_{\Delta 2\text{-}354})$$

$$= (1.996)\ (298)\ [\ln(141.98/21.32)]$$

$$= 1.10 \text{ kcal/mol.}$$

The destabilizing effect caused by elevated external K^+ is:

$$\Delta G_{WT} - \Delta G_{\text{high } K^+} = -RT\ln(\beta_{WT}/\beta_{\text{high } K^+})$$

$$= RT\ln(\tau_{\text{high } K^+}/\tau_{WT})$$

$$= (1.996)\ (298)\ [\ln(141.98/60.50)]$$

$$= 0.55 \text{ kcal/mol.}$$

The saturated deactivation rates are consistent with a destabilization of NH_2 terminus binding to its receptor site by approximately 50%, or 0.55 kcal/mol.

Modification of G546C in the S4–S5 Linker Phenocopies the NH_2 Terminus Deletion

We tested the hypothesis that the HERG NH_2 terminus interacts with the S4–S5 linker in a manner analogous to the interaction of the *Shaker* NH_2 terminus with the corresponding residues at the internal mouth of the pore. We used the substituted cysteine modification approach to interfere with binding, and assayed for a deactivation phenocopy of Δ2-354 (Fig. 5). At several sites, introduction of a cysteine increased deactivation rates (Fig. 5 *A*, *open bars*). Deactivation rates of mutants R541C, S543C, G546C, and A547C were not significantly different from those of wild type (Fig. 5 *A*, *filled bars*), information important in ruling out the possibility that subsequent modification simply enhances a mutant effect introduced by the cysteine. Of these cysteine mutants with wild-type deactivation kinetics, only G546C showed significant alteration of deactivation rate when modified by NEM (Fig. 5, *B* and *C*). A comparison of deactivation τ's indicates that modification of G546C mimics the effect of Δ2-354 (Fig. 5 *D*). When G546C is combined with the Δ2-354, no further modulation of deactivation τ's are observed with NEM modification, indicating that modification of the S4–S5 linker and

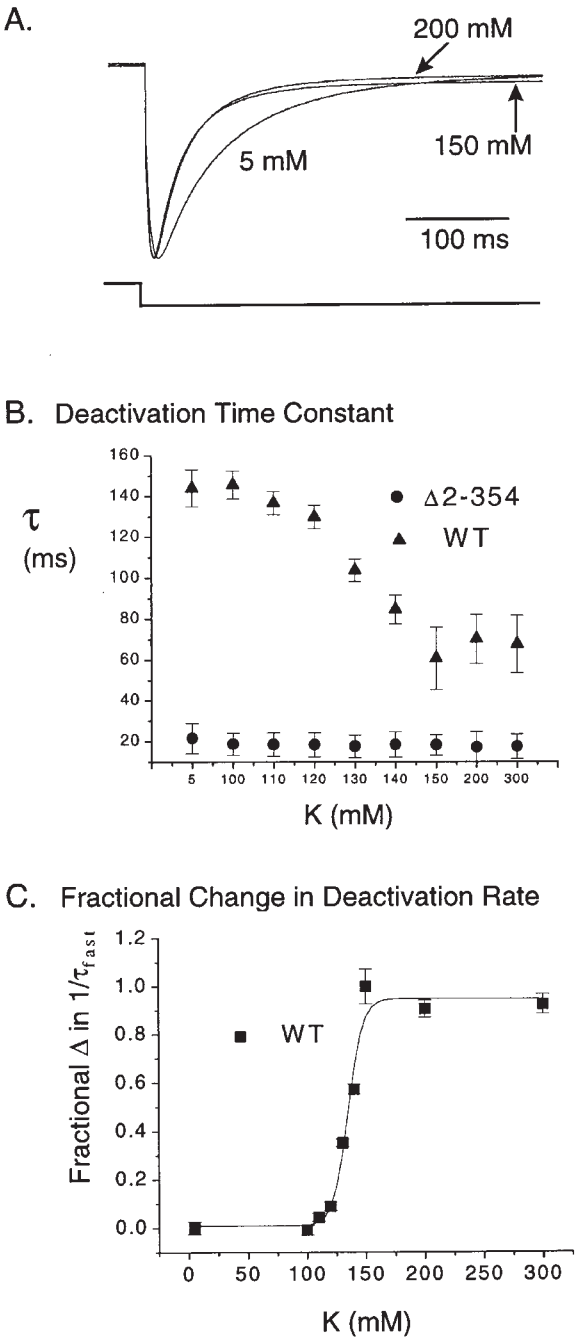

FIGURE 4. Deactivation rate in HERG channels increases with elevated external K^+. (*A*) Scaled tail currents from WT channels in 5, 150, and 200 mM external K^+. Currents were evoked at −100 mV subsequent to a 3-s step to 60 mV. (*B*) Deactivation time constants at various external K^+ concentrations for both WT ($n = 6$) and Δ2-354 ($n = 5$) channels for tail currents evoked as described in *A*. Tail currents were fit with a single exponential function in this case because, at −100 mV, the fast component accounts for >90% of the current. (*C*) The change in deactivation rate ($1/\tau$) with increasing external K^+ exhibits a saturating dose–response behavior with a Hill coefficient of 5.36 ± 0.69. At −100 mV, the forward (activation) rate is negligible and most of the deactivating current is described by the fast deactivation τ (Table I) so the deactivation rate $\cong 1/\tau_{fast}$. As shown, deactivation rate increased in a dose-dependent manner with increased external K^+ ions. These data were fitted with the Hill equation: $\ln[(1 - S')/S'] = -n(\ln K - \ln L)$, where $S' = S/S_0$ is the fraction of sites occupied by the ligand, S is the number of sites occupied, S_o is the total number of sites available, K is the dissociation constant of the ligand, L is the ligand concentration, and n is the Hill coefficient. We determine S' using the formula $(k - k_5)/(k_{300} - k_5)$, where k is the deactivation rate ($1/\tau$ at −100 mV) at any given external potassium concentration, k_5 is the rate at 5 mM $[K]_o$, and k_{300} the rate at 300 mM $[K]_o$. The S' values at different $[K]_o$ (i.e., L) were plotted as fractional increase of deactivation rate in *C*. The resulting sigmoidal dose–response curve was then fitted with the Hill equation indicated above to obtain the Hill coefficient.

deletion of the NH_2 terminus disrupt the same process. The wild-type HERG channel was unaffected by the NEM treatment (Fig. 5 *D*), indicating that endogenous cysteines, even if modified by NEM, play no role in deactivation kinetics. Modification of G546C also slows C-type inactivation to the same extent as does HERG Δ2-354 (Fig. 5 *E*). These data show that the ability of the NH_2 terminus to slow deactivation and promote C-type inactivation is disrupted by modification of G546C and they suggest that regulation of these gating processes under normal circumstances involves an interaction between the NH_2 terminus and the S4–S5 linker.

A Small Deletion Distinguishes Domains Regulating Deactivation and Inactivation

Our initial attempts to localize the domain regulating control of deactivation led to the surprising result that different regions of the NH_2 terminus were responsible for controlling deactivation and inactivation. Based on the location of a convenient restriction site and a meeting report of a small deletion increasing deactivation rate (Schönherr et al., 1997), we generated a construct lacking amino acid residues 2–12 (Δ2-12; Fig. 6 *A*). We found that the deactivation rates of Δ2-12 and Δ2-354 were indistinguishable (Fig. 6 *B*). In contrast, Δ2-12 did not exhibit the dramatic slowing of inactivation characteristic of Δ2-354 (Fig. 6 *C*). This result suggests that the extreme NH_2 terminus is required for the slowing of deactivation, but not for the promotion of C-type inactivation. However, as shown in the previous figure, modification of G546C in the S4–S5 loop disrupts both processes, as if they both depend on the binding of the NH_2 terminus to a site near that region (compare Fig. 5, *D* and *E*).

DISCUSSION

Similarities between NH_2 Terminus Regulation of Deactivation in HERG and N-Type Inactivation in Shaker

The goal of this study was to explore the mechanism by which the NH_2 terminus modulates deactivation rate in HERG channels. We tested the hypothesis that the NH_2 terminus slows deactivation by a foot-in-the-door mechanism similar to N-type inactivation in *Shaker* (Demo

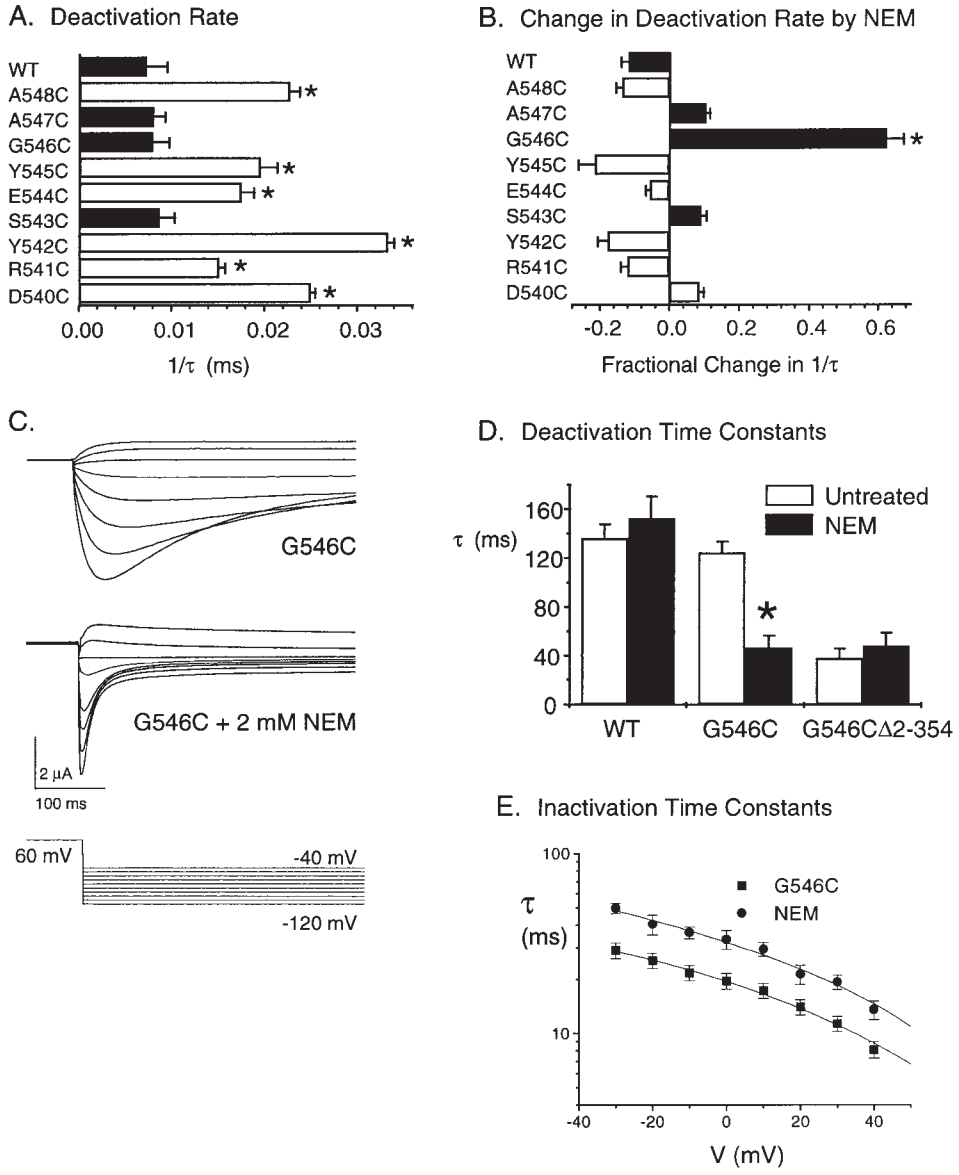

FIGURE 5. NEM modification of the S4–S5 linker mimics the NH_2 terminus deletion. (*A*) Deactivation rates for cysteine substitutions at each position within the S4–S5 linker region. The open bars with the asterisks indicate the positions where cysteine substitution significantly speeds deactivation rate ($n \geq 3$ for each mutant). Note that deactivation rate is not significantly altered by G546C. (*B*) Fractional change of deactivation rate by NEM modification for all the cysteine substitutions. Positive numbers indicate increased rate. *Dramatic effect on the G546C mutant. (*C*) Families of tail currents from G546C channels before and after NEM modification. (*D*) Summary of effects of NEM modification on WT, G546C, and G546C Δ2-354 channels. Time constants were determined by fitting tail currents to a single exponential function because, at −100 mV, the fast component accounts for >90% of the current. The first pair of bars indicates that NEM modification does not significantly affect deactivation time constants for wild-type channels. The second set of bars shows marked effect of NEM modification on G546C mutant. The third set of bars shows that modification of G546C Δ2-354 does not further accelerate the deactivation rate, indicating that NEM and deletion of the NH_2 terminus disrupt the same process ($n = 6$ for each construct). (*E*) Inactivation time constants measured from G546C channels show that modification of the S4–S5 linker results in slower C-type inactivation ($n = 7$).

and Yellen, 1991) and block in K^+ channels by tetraethylammonium and its derivatives (Armstrong, 1969, 1971), which also slow deactivation. We found that the ability of the NH_2 terminus to slow deactivation was reduced by elevating external K^+ concentration consistent with a 50% reduction of the free energy of binding of the NH_2 terminus and a knock-off effect by which K^+ influx disrupts the binding of the NH_2 terminus to the internal mouth of the pore.

We asked whether the S4–S5 loop serves as a binding site for the NH_2 terminus, as it does in *Shaker* channels (Isacoff et al., 1991; Holmgren et al., 1996), by covalently modifying cysteine residues introduced within this region. Modification of one such mutant (G546C), which itself had a wild-type phenotype, produced a phenocopy of Δ2-354, as if the cysteine modification introduced a steric hindrance to the binding of the NH_2 terminus. In these ways, the regulation of deactivation by the NH_2 terminus in HERG bears considerable similarity to N-type inactivation in *Shaker* channels.

Differences between NH_2 Terminus Regulation of Deactivation in HERG and N-Type Inactivation in Shaker

Despite the similarities with N-type inactivation in *Shaker*, several other aspects of NH_2 terminus function appear to be specific to the regulation of deactivation in HERG. Inactivation in HERG occurs by a single exponential

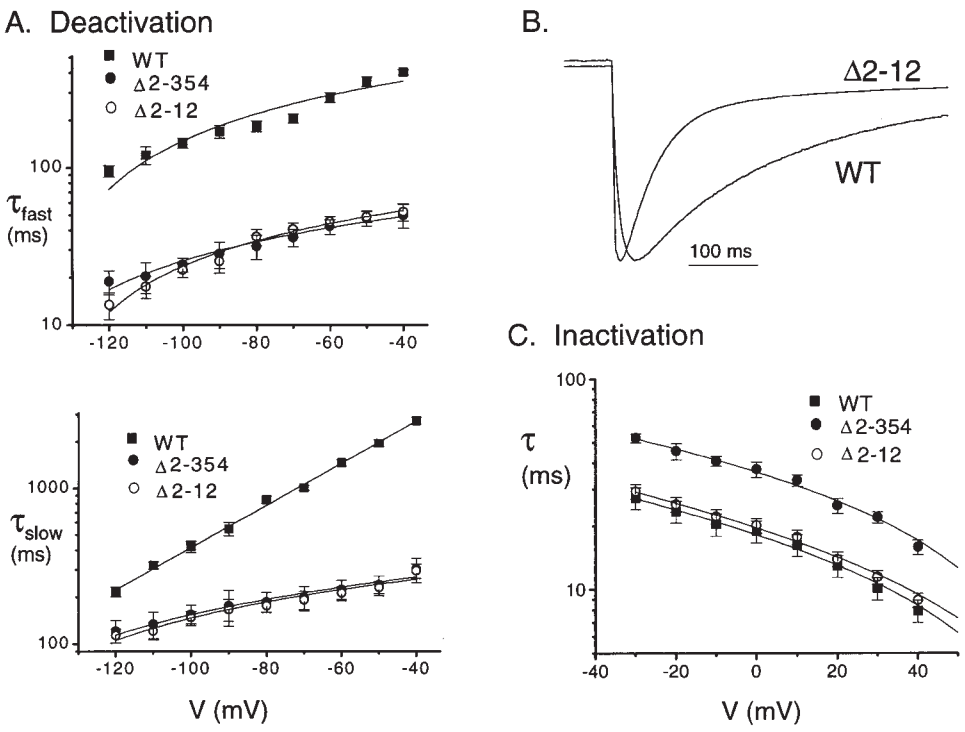

FIGURE 6. Domains regulating deactivation and inactivation are spatially distinct within the NH_2 terminus. (*A*) Scaled tail currents from Δ2-12 and WT channels show that the small deletion increases deactivation rate. (*B*) Fast and slow deactivation time constants for WT ($n > 10$), Δ2-354 ($n > 10$), and Δ2-12 ($n = 6$) channels indicate that the two deletions have similar effects on deactivation kinetics. (*C*) Inactivation time constants for HERG WT ($n > 10$), Δ2-354 ($n > 10$), and Δ2-12 ($n = 6$) show that the small deletion does not significantly alter the inactivation rate ($P > 0.6$ at 0.05 confidence interval for each voltage).

process and is essentially removed by point mutations affecting C-type inactivation (Smith et al., 1996; Suessbrich et al., 1997; Herzberg et al., 1998). As is apparent in Fig. 3 *A*, there is no sign of residual N-type inactivation when C-type inactivation is removed, even though the modulation of deactivation by the NH_2 terminus remains intact in these mutant channels. Nor is there any indication of block, which would be associated with an increase in current amplitude when the NH_2 terminus is removed. Thus, the NH_2 terminus stabilizes the open state by a mechanism that apparently does not involve block and yet is sensitive to an increase in the concentration of the permeant species (see Scheme II, where O_N is a conducting state bound by the NH_2 terminus). If the destabilization of the NH_2 terminus by increased extracellular K^+ is indeed due to increased ion flux through the pore, this implies that pore occlusion is not a requirement for the knock-off effect. Single channel studies may be required to fully resolve this point.

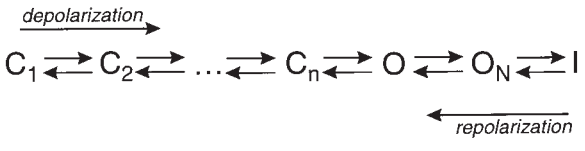

(SCHEME II)

The deactivating tails of wild-type HERG channels exhibit two time constants, with the slower of the two more steeply voltage dependent (Fig. 1 *C*). By analogy with the voltage-dependent block of Ca^{2+}-activated K^+channels by charybdotoxin (MacKinnon and Miller, 1988), at least part of the voltage dependence of this process may derive from the sensitivity of NH_2 terminus dissociation to changes in the K^+ driving force. This would explain why such a steeply voltage-dependent component is not observed when the NH_2 terminus has been deleted. Based on Scheme II, the two time constants would be associated with transitions in the closing path. Deleting the NH_2 terminus could directly or allosterically affect both processes; alternatively, removing the stabilizing influence of the NH_2 terminus could speed subsequent transitions via mass action (more channels available to move from O to C or from C to a more remote C state at any given time). Further experiments will be required to distinguish among these and other possibilities.

Another argument that the HERG NH_2 terminus has a distinct mode of action compared with N-type inactivation is a difference in the stoichiometry of NH_2-terminal action suggested by heteromeric assembly of isoforms of Merg1, the mouse ortholog to HERG (Lees-Miller et al., 1997; London et al., 1997). Merg1a is 96% identical to HERG, and their currents are indistinguishable when expressed in oocytes. Isoform Merg1b is identical in sequence to Merg1a except for its novel, short NH_2 terminus. Although they express poorly, homomeric Merg1b channels clearly exhibit a fast deactivation phenotype. When coexpressed, Merg1a and Merg1b heteromers exhibit fast deactivation rates that are similar to those of the Merg1b isoform expressed alone and ~10-fold faster than Merg1a deactivation (London et al., 1997). These results argue against a

Shaker-type ball-and-chain model, in which a single NH_2-terminal domain is required to mediate inactivation, and most (15/16) channels assembled from an equal mixture of *Shaker* wild-type and N-deleted subunits have at least one NH_2 terminus (MacKinnon et al., 1993). If the Merg1a NH_2 terminus acted by a similar mechanism, except that in this case the deactivation rate would be determined by the dissociation of the NH_2 terminus, then even a single Merg1a subunit in a tetrameric channel would slow deactivation; most of the channels, therefore, would exhibit the slow deactivation phenotype. Instead, the majority of Merg1a/1b channels exhibit the fast deactivation phenotype, arguing that more than one and possibly all four NH_2 termini are required to slow deactivation. Alternatively, a single short NH_2 terminus may inhibit the slowing of deactivation by the longer NH_2 termini and provide a regulatory mechanism by which heteromeric association with Merg1b dominantly regulates deactivation kinetics. A similar mechanism has recently been attributed to the NIP domain, a region of a beta subunit that inhibits NH_2-terminal function of the *Shaker* channels with which it coassembles (Roeper et al., 1998). Experiments addressing the stoichiometry of NH_2-terminal function in HERG and Merg are currently under way.

Functional Domains within the NH_2 Terminus

Our results also suggest that modulation of deactivation and inactivation require the involvement of different subdomains of the NH_2 terminus, in contrast to the apparent causal relationship for NH_2-terminal block and enhancement of C-type inactivation in *Shaker* channels (Baukrowitz and Yellen, 1995). Thus, the mechanisms by which the NH_2 terminus regulates C-type inactivation in HERG and *Shaker* channels may differ. On the other hand, the promotion of C-type inactivation in *Shaker* has been inferred from NH_2-terminal deletions (Hoshi et al., 1990, 1991) and, to our knowledge, has never been directly attributed to the extreme NH_2 terminus or the "ball" domain peptide. This raises the possibility that different NH_2-terminal domains regulate deactivation and C-type inactivation in *Shaker* as in HERG channels. It is interesting that the regulation of both deactivation and inactivation in HERG involve the NH_2 terminus and the S4–S5 loop, as if the interaction of these regions is essential for bringing both functional domains of the NH_2 terminus into proximity with their targets in the hydrophobic core.

Li et al. (1997) have described an oligomerization domain in HERG that mediates tetrameric assembly of the isolated NH_2 terminus in solution. Although this region has not been mapped within the NH_2 terminus, we can speculate that such an interaction might be important for the function of the NH_2 terminus in slowing deactivation. This finding is consistent with the model that more than one NH_2 terminus is involved in the deactivation process.

Our results suggest a mechanism by which a discrete domain within the NH_2 terminus slows deactivation by stabilizing the open state. This domain is separable from another region that promotes C-type inactivation. The binding of the NH_2 terminus to a region near the S4–S5 loop is essential for both interactions. Multiple NH_2 termini are apparently involved in regulating deactivation, although the nature of this coordinate action remains to be elucidated. Future functional and structural experiments will be required to fully understand the complexities by which the NH_2 terminus regulates various aspects of channel gating in homomeric and heteromeric channel assemblies.

We thank Richard Schell and Heather Matthews for technical help, Drs. Ebru Aydar, Janet Branchaw, Robert Fettiplace, Craig January, Gareth Tibbs, and Zhengfeng Zhou for their comments on a previous version of the manuscript, and Dr. Cynthia Czajkowski for advice on cysteine mutagenesis and modification.

This work was supported by NIH grant HL-55973, a gift from the Bayer Corporation, a National Science Foundation CAREER award, and an American Heart Association (AHA) Established Investigator award (to G.A. Robertson), as well as by predoctoral fellowships from AHA-Wisconsin (to J. Wang and M.C. Trudeau).

Original version received 10 June 1998 and accepted version received 21 September 1998.

REFERENCES

Armstrong, C.M. 1966. Time course of TEA induced anomalous rectification in the squid giant axons. *J. Gen. Physiol.* 50:491–503.

Armstrong, C.M. 1969. Inactivation of the potassium conductance and related phenomena caused by quaternary ammonium ion injection in squid axons. *J. Gen. Physiol.* 54:553–575.

Armstrong, C.M. 1971. Interaction of tetraethylammonium ion derivatives with the potassium channels of giant axons. *J. Gen. Physiol.* 58:413–437.

Baukrowitz, T., and G. Yellen. 1995. Modulation of K^+ current by frequency and external $[K^+]$: a tale of two inactivation mechanisms. *Neuron.* 15:951–960.

Demo, S.D., and G. Yellen. 1991. The inactivation gate of the *Shaker* K^+ channel behaves like an open-channel blocker. *Neuron.* 7: 743–753.

Herzberg, I.M., M.C. Trudeau, and G.A. Robertson. 1998. Transfer of inward rectification and E-4031 sensitivity from HERG to M-eag. *J. Physiol. (Camb.)*. 511:3–14.

Holmgren, M., M.E. Jurman, and G. Yellen. 1996. N-type inactivation and the S4–S5 region of the *Shaker* K channel. *J. Gen. Physiol.* 108:195–206.

Hoshi, T., W.N. Zagotta, and R.W. Aldrich. 1990. Biophysical and molecular mechanisms of *Shaker* potassium channel inactivation. *Science*. 250:533–538.

Hoshi, T., W.N. Zagotta, and R.W. Aldrich. 1991. Two types of inactivation in *Shaker* K^+ channels: effects of alterations in the carboxy-terminal region. *Neuron*. 7:547–556.

Isacoff, E.Y., Y.H. Jan, and L.Y. Jan. 1991. Putative receptor for the cytoplasmic inactivation gate in the *Shaker* K channel. *Nature*. 353:86–90.

Landt, O., H.P. Grunert, and U. Hahn. 1990. A general method for rapid site-directed mutagenesis using the polymerase chain reaction. *Gene*. 96:125–128.

Lees-Miller, J.P., C. Kondo, L. Wang, and H.J. Duff. 1997. Electrophysiological characterization for an alternatively processed ERG K channel in mouse and human hearts. *Circ. Res.* 81:719–726.

Li, X., J. Xu, and M. Li. 1997. The human Δ1261 mutation of the HERG potassium channel results in a truncated protein that contains a subunit interaction domain and decreases the channel expression. *J. Biol. Chem.* 272:705–708.

London, B., M.C. Trudeau, K.P. Newton, A.K. Beyer, N.G. Copeland, D.J. Gilbert, N.A. Jenkins, C.A. Satler, and G.A. Robertson. 1997. Two isoforms of the mouse Ether-à-go-go-related gene coassemble to form channels with properties similar to the rapidly activating component of the cardiac delayed rectifier K current. *Circ. Res.* 81:870–878.

London, B., E. Aydar, C.M. Lewarchik, J.S. Seibel, C.T. January, and G.A. Robertson. 1998. N- and C-terminal isoforms of HERG in the human heart. *Biophys. J.* 74:*A*26. (Abstr.)

MacKinnon, R., and C. Miller. 1988. Mechanism of charybdotoxin block of the high conductance, Ca^{2+}-activated K^+ channel. *J. Gen. Physiol.* 91:335–349.

MacKinnon, R., R.W. Aldrich, and A.W. Lee. 1993. Functional stoichiometry of *Shaker* potassium channel inactivation. *Science*. 262: 757–759.

Pajor, A.M., B.A. Hirayama, and E.M. Wright. 1992. Molecular biology approaches to comparative study of Na(+)-glucose cotransport. *Am. J. Physiol.* 263:R489–R495.

Roeper, J., S. Sewing, Y. Zhang, T. Sommer, S.G. Wanner, and O. Pongs. 1998. NIP domain prevents N-type inactivation in voltage-gated potassium channels. *Nature*. 391:390–393.

Sanguinetti, M.C., C. Jiang, M.E. Curran, and M.T. Keating. 1995. A mechanistic link between an inherited and an acquired cardiac arrhythmia: HERG encodes the I_{Kr} potassium channel. *Cell*. 81: 299–307.

Sanguinetti, M.C., and N.K. Jurkiewicz. 1990. Two components of cardiac delayed rectifier K^+ current. *J. Gen. Physiol.* 96:195–215.

Schönherr, R., and S.H. Heinemann. 1996. Molecular determinants for activation and inactivation of HERG, a human inward rectifier potassium channel. *J. Physiol. (Camb.)*. 493:635–642.

Schönherr, R., R. Meyer, Y. Kubo, and S.H. Heinemann. 1997. Gating kinetics of HERG K^+ channels is determined by the N-terminal domain and protein phosphorylation. *Biophys. J.* 72:*A*342. (Abstr.)

Shibasaki, T. 1987. Conductance and kinetics of delayed rectifier potassium channels in nodal cells of the rabbit heart. *J. Physiol. (Camb.)*. 387:227–250.

Smith, P.L., T. Baukrowitz, and G. Yellen. 1996. The inward rectification mechanism of the HERG cardiac potassium channel. *Nature*. 379:833–836.

Spector, P.S., M.E. Curran, A. Zou, M.T. Keating, and M.C. Sanguinetti. 1996. Fast inactivation causes rectification of the I_{Kr} channel. *J. Gen. Physiol.* 107:611–619.

Suessbrich, H., R. Schönherr, S.H. Heinemann, F. Lang, and A.E. Busch. 1997. Specific block of cloned Herg channels by clofilium and its tertiary analog LY97241. *FEBS Lett.* 414:435–438.

Trudeau, M.C., J.W. Warmke, B. Ganetzky, and G. Robertson. 1995. HERG, a human inward rectifier in the voltage-gated potassium channel family. *Science*. 269:92–95.

Wang, S., S. Liu, M.J. Morales, H.C. Strauss, and R.L. Rasmusson. 1997. A quantitative analysis of the activation and inactivation kinetics of HERG expressed in *Xenopus* oocytes. *J. Physiol. (Camb.)*. 502:45–60.

Warmke, J.W., and B. Ganetzky. 1994. A family of potassium channel genes related to *eag* in *Drosophila* and mammals. *Proc. Natl. Acad. Sci. USA*. 91:3438–3442.

Zagotta, W.N., T. Hoshi, and R.W. Aldrich. 1990. Restoration of inactivation in mutants of *Shaker* potassium channels by a peptide derived from ShB. *Science*. 250:568–570.

Zeng, J., K.R. Laurita, D.S. Rosenbaum, and Y. Rudy. 1995. Two components of the delayed rectifier K^+ current in ventricular myocytes of the guinea pig type. Theoretical formulation and their role in repolarization. *Circ. Res.* 77:140–152.

Zhou, Z., Q. Gong, B. Ye, Z. Fan, J.C. Makielski, G.A. Robertson, and C.T. January. 1998. Properties of HERG channels stably expressed in HEK 293 cells studied at physiological temperature. *Biophys. J.* 74:230–241.